Biochemical and Biophysical Research Communications 391 (2010) 152–158

Contents lists available at ScienceDirect

Biochemical and Biophysical Research Communications

journal homepage: www.elsevier.com/locate/ybbrc

Differential expression of P-type ATPases in intestinal epithelial cells: Identification of putative new *atp1a1* splice-variant

Miguel A. Rocafull *, Luz E. Thomas, Girolamo J. Barrera, Jesús R. del Castillo

Lab. Fisiología Molecular, Centro de Biofísica y Bioquímica, Instituto Venezolano de Investigaciones Científicas (IVIC), Apartado 20632, Caracas 1020-A, Venezuela

ARTICLE INFO

Article history:
Received 2 November 2009
Available online 10 November 2009

Keywords:
ATNA
ATP1A1
ATP12A
PCR
PMCA
SERCA

ABSTRACT

P-type ATPases are membrane proteins that couple ATP hydrolysis with cation transport across the membrane. Ten different subtypes have been described. In mammalia, 15 genes of P-type ATPases from subtypes II-A, II-B and II-C, that transport low-atomic-weight cations (Ca^{2+}, Na^+, K^+ and H^+), have been reported. They include reticulum and plasma-membrane Ca^{2+}-ATPases, Na^+/K^+-ATPase and H^+/K^+-ATPases. Enterocytes and colonocytes show functional differences, which seem to be partially due to the differential expression of P-type ATPases. These enzymes have 9 structural motifs, being the phosphorylation (E) and the Mg^{2+}ATP-binding (H) motifs the most preserved. These structural characteristics permitted developing a Multiplex-Nested-PCR (MN-PCR) for the simultaneous identification of different P-type ATPases. Thus, using MN-PCR, seven different cDNAs were cloned from enterocytes and colonocytes, including SERCA3, SERCA2, Na^+/K^+-ATPase α1-isoform, H^+/K^+-ATPase α2-isoform, PMCA1, PMCA4 and a cDNA-fragment that seems to be a new cassette-type splice-variant of the *atp1a1* gen. PMCA4 in enterocytes and H^+/K^+-ATPase α2-isoform in colonocytes were differentially expressed. This cell-specific expression pattern is related with the distinctive enterocyte and colonocyte functions.

Introduction

The P-type ATPases constitute a family of integral membrane proteins, which actively transport cations or amino-phospholipids across membrane, coupling this process with ATP-hydrolysis [1,2]. They are also denominated E1–E2 ATPases because they follow a characteristic reaction cycle between two different conformational states: E1 and E2 [2]. During this catalytic cycle, γ-phosphate group from ATP is transferred to a specific aspartyl-residue of the enzyme, generating a phospho-enzyme intermediary, which is characteristic of all P-type ATPases [1,2]. This catalysis is Mg^{2+}-dependent and inhibited by vanadate [1,2].

At least, ten different subtypes of P-type ATPases have been described [2,3]. The subtypes II-A, II-B and II-C are the only, described in mammalia, that transport low-atomic-weight cations [2,3]. Subtype II-A is integrated by Ca^{2+}-ATPases from sarco/endo-plasmatic reticulum (SERCA) and Golgi apparatus (PMR). Three isoforms of SERCA (SERCA1-3) and two isoforms of PMR (PMR1-2) have been identified. Subtype II-B includes Ca^{2+}-ATPases from plasma membrane, existing four PMCA isoforms (PMCA1-4). Subtype II-C is mainly integrated by Cation/K^+-ATPases, which include four isoforms of the Na^+/K^+-ATPase (ATP1A1-4) and two isoforms of H^+/K^+-ATPase, the gastric (ATP4A) and non-gastric (ATP12A or ATP1AL1) isoforms [2,3]. Until now, only SERCA3, PMCA1, PMCA4, ATP1A1 and ATP12A have been identified in intestinal epithelia [4–6]. However, the genetic identity of certain P-type ATPase activities, described in intestinal epithelial cells [7,8], has not been elucidated.

The catalytic subunit of P-type ATPases (α-subunit) has 6–10 α-helical transmembrane segments (M1–M10) alternated with cytosolic and extra-cytosolic loops [1,2]. The cytosolic B-loop, between M2 and M3, contains the phosphatase domain (A-domain). The cytosolic C-loop, located between M4 and M5, includes the kinase and the nucleotide-binding domains (P- and N-domains, respectively) [2]. Additionally, P-type ATPases have nine highly-preserved structural motifs, denoted with letters from A to I, which are arranged from N- to C-terminal as follows: "A" ($PGDX_{10}PAD$), "B" (TGES), "C" (GX_9G), "D" (P[E/V/I/C]GL), "E" (ICSDKTGTLT), "F" (KGAP), "G" ($DPPRX_6[I/V]X_6GX_6TGDX_4A$), "H" (TGDGVNDSPALKKAD), and "I" (A[K/R]XAAD) [1–3]. The C-loop has five of them, including the two most preserved: E (phosphorylation-motif) and H (Mg^{2+}-ATP binding motif) [1–3]. The E-motif includes the essential Asp residue phosphorylated during the catalytic cycle [1,2].

P-type ATPases are quasi-ubiquitously distributed into phylogenetic scale [1–3]. They are essential for several physiological processes, have been involved in some pathologies and are important therapeutic-targets [2,9,10]. In intestinal epithelia, P-type ATPases play essential roles in absorptive and secretory processes [6–8,11–13]. Moreover, enterocytes and colonocytes

* Corresponding author. Fax: +58 212 5041093.
E-mail addresses: mrocaful@ivic.ve, miguelrocafull@hotmail.com (M.A. Rocafull).

0006-291X/$ - see front matter © 2009 Elsevier Inc. All rights reserved.
doi:10.1016/j.bbrc.2009.11.023

show some functional differences which seem to be partially due to the differential expression of these enzymes [8,12]. The recognition of cell-specific expression pattern (or the identification of new P-type ATPases) is essential for the understanding of mechanisms involved in intestinal function. Thus, their detection by specific and sensitive techniques becomes relevant.

Degenerate-PCR, based in conserved amino-acid sequences, has been successfully employed to clone several genes [14,15]. This technique requires two target amino-acid sequences, of at least 6-amino-acid long, which must be highly preserved and adequately located at the protein primary structure [14]. P-type ATPases only have two motifs that fulfill these requirements: the E- and H-motifs.

In this paper, expression of P-type ATPases from subtypes II is determined in enterocytes and colonocytes by a degenerate-PCR variant denominated Multiplex-Nested-PCR (MN-PCR). It combines successive RT-PCR and Nested-PCR to enhance specificity and sensibility. Both PCRs employed degenerate primers, which recognize the cDNA-segments that encode the E- and H-motifs. Additionally, the size of the PCR-products was specific for each P-type ATPase.

Materials and methods

Present work was approved by IVIC Bioethical Committee and carried out in accordance with EC Directive 86/609/EEC for animal experiments.

Materials. Agarose, Trizol Reagent, Thermoscript RT-PCR System, HiFi Platinum Taq DNA Polymerase, TOPO TA Cloning Kit for Sequencing, DNA weight markers, antibiotics, culture mediums and custom primers were from Invitrogen. Thermocyclers, electrophoretic reagents and devices were from Bio-Rad and MJ Research. Real-time master mix was from Fynnzymes. Wizard Purification Kits and EcoRI were from Promega. The other products were from SIGMA, MERCK and Thermo EC.

Intestinal cell isolation. Epithelial cells from small intestine and distal colon were isolated from guinea-pig as described [12,16].

RNA isolation and cDNA synthesis. Total RNA was prepared from intestinal epithelial cells processing 7.5×10^6 cells per 1 ml of Trizol Reagent. Poly(A)$^+$-RNA was purified by Oligo(dT)-cellulose chromatography [17]. Single-strand cDNA was synthesized from 3 μg of total RNA or 0.5 μg of Poly(A)$^+$-RNA, using ThermoScript RT-PCR System with Oligo$(dT)_{20}$ as primers. Manufacturer indications were followed.

Design of degenerate primers. In a degenerate-PCR, primer degeneracy determines the number of recognizable target DNA sequences and the variability in melting-temperature (T_m) of the oligonucleotide mixture. These parameters considerably affect the specificity and sensibility of the PCR technique [14,18]. To decrease oligonucleotide degeneracy, primers were designed from consensus cDNA sequence of several P-type ATPases. This designing considers the codons phylogenetically preserved in each position instead of the specie-codon-usage described by Wada et al. [19]. Only subtypes II-A, II-B and II-C were considered because they are the unique subtypes, reported in mammalia, which can transport cations of low atomic weight. In this order, 96 cDNA sequences of P-type ATPases from several species were aligned through ClustalX Multiple Alignment Program v1.81 [20], being the consensus sequence determined. Forward and reverse primers were designed from the segments which encode E- and H-motifs, respectively (Fig. 1A). Sequences and other primer details are shown in Fig. 1B. Oligonucleotide melting-temperature (T_m) was estimated as described [14].

Degenerate polymerase chain reactions. RT-PCR was carried out using 2 μl of cDNA synthesis reaction as template and 100 nM/oligonucleotide of each outer-primer (OFP and ORP). Optimal cycling parameters were 94 °C for 2 min; followed by 5 low-astringency cycles of 94 °C for 1 min, 45 °C for 1 min and 68 °C for 2 min; followed by 35 cycles of 94 °C for 1 min, 54 °C for 1 min and 68 °C for 2 min; and a final step of 68 °C for 10 min. Nested-PCR was performed employing 1 μl of 1000-fold diluted RT-PCR product as template and 50 nM/oligonucleotide of each inner-primer (IFP and IRP). Optimal cycling parameters were 94 °C for 2 min; followed by 20 cycles of 94 °C for 1 min, 56 °C for 1 min and 68 °C for

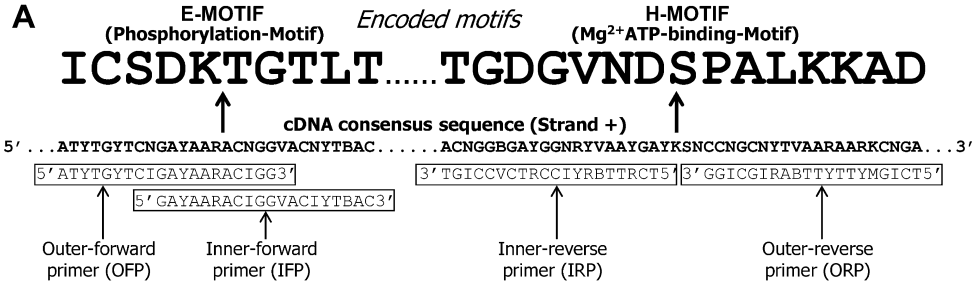

B

Primer	Sequence	Tm range of the mixture (°C)	Degeneracy degree	Number of different oligonucleotides	Use
OFP	5'-ATYTGYTCIGAYAARACIGG-3'	52-64	256	16	RT-PCR
ORP	5'-TCIGMYTTYTTBARIGCIGG-3'	52-68	3072	48	RT-PCR
IFP	5'-GAYAARACIGGVACIYTBAC-3'	55-66	1152	72	Nested-PCR
IRP	5'-TCRTTBRYICCRTCVCCIGT-3'	54-70	2304	144	Nested-PCR

C

Sub-type	ATPase	PCR-product estimated sizes (bp) RT-PCR	Nested-PCR	n
II-A	PMR(1-2)	929-968	896-935	5
II-A	SERCA(1-3)	1094-1106	1061-1073	20
II-B	PMCA(1-4)	1007-1013	974-980	12
II-C	Na^+/K^+-ATPase α(1-4)	1064-1076	1031-1043	56
II-C	H^+/K^+-ATPase α(1-2)	1070	1037	3

Fig. 1. MN-PCR strategy. (A) Design of degenerate primers from consensus cDNA sequence of 96 P-type ATPases, belong to subtypes II-A, II-B and II-C. (B) Characteristics of each degenerate primer. (C) Estimated size for RT- and Nested-PCR products for each P-type ATPase, based on GenBank database. The number of sequences used to estimate PCR-product sizes is identified by "*n*".

2 min; and a final step of 68 °C for 10 min. Both PCR reactions were carried out in a final volume of 50 μl with 1× HiFi PCR Buffer, 2.32 mM $MgSO_4$, 400 μM of each dNTP and 2 U of HiFi Platinum Taq DNA Polymerase, using a GeneCycler as thermocycler. Size of expected PCR-products is specific for each cDNA (Fig. 1C), given that E and H-motifs delimit a segment whose size is characteristic for each P-type ATPase.

Specific RT-PCRs and qRT-PCRs for PMCA4 and ATP12A. Differential expression of PMCA4 and ATP12A was verified by RT-PCR from 0.5 μg of Poly(A)$^+$-RNA, employing ThermoScript RT-PCR System. Their expression was quantified by real-time RT-PCR (qRT-PCR) as triplicate from three different total RNA preparations, using 1× Master Mix SYBR in a Chromo4 Real Time PCR thermal cycler. Primers and annealing temperatures are shown in Fig. 3A. Manufacturer instructions were followed.

Electrophoretic analysis of PCR-products. PCR-products were run onto 4% polyacrylamide gel electrophoresis (4% PAGE) with 10 mA of constant current at 10 °C for 12 h (buffer was renewed at 6 h) or agarose gel electrophoresis (AGE) as indicated. Gels were stained with ethidium bromide [17], visualized on DyNa Light UV-transilluminator and photographed with DC256 Kodak digital camera. Images were analyzed through "Kodak Digital Science

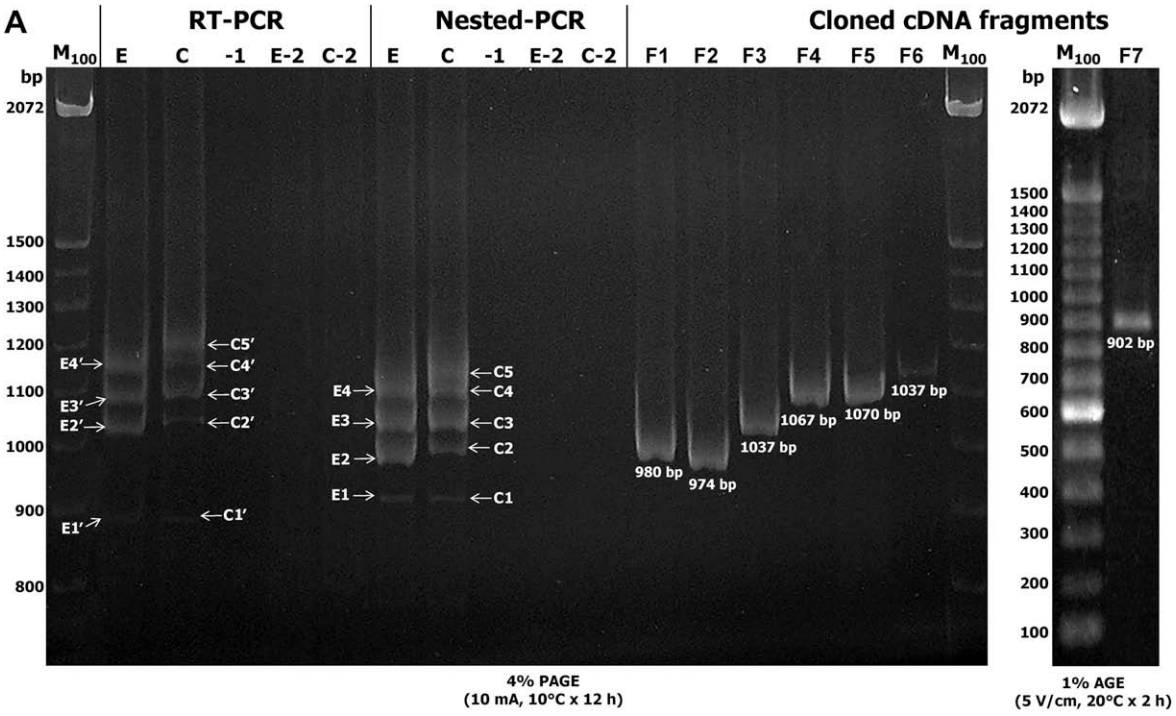

B

cDNA Fragment	Size (bp)	Origin band	ATPase	GenBank Accession Number	blastn (% of Identity)	blastp (% of identity / % of homology)
F1	980	E2 and C2	PMCA1	EF489480	**95%** Human *atp2b1* (gi:48255944)	**99%/99%** Human PMCA1 (gi:48255945)
F2	974	E2	PMCA4	EF489481	**89%** Human *atp2b4* (gi:48255956)	**91%/95%** Human PMCA4 (gi:48255957)
F3	1037	E3 and C3	ATP1A1	EF489488	**90%** Orangutan *atp1a1* (gi:55726661)	**97%/99%** Human Na^+/K^+ ATPase α1 (gi:29791449)
F4	1067	E4 and C4	SERCA2	EF489482	**88%** Human *atp2a2* (gi:27886537)	**97%/98%** Rat SERCA2 (gi:203059)
F5	1070	E4 and C4	SERCA3	EF489483	**96%** Human *atp2a3* (gi:23273018)	**93%/94%** Human SERCA3 (gi:28373103)
F6	1037	C5	ATP12A	Q64392	**100%** Guinea pig *atp12a* (gi:431136)	**100%/100%** Guinea pig H^+/K^+ ATPase α2 (gi:5915706)
F7	902	E1 and C1	ATNA	EF489487	**79%** Orangutan *atp1a1* (gi:55726661)	**85%/87%** Human Na^+/K^+ ATPase α1 (gi:29791449)

Fig. 2. Electrophoresis and cloning of PCR-products. (A) RT-PCR (left panel) and Nested-PCR (middle panel) products were run onto 4% PAGE at 10 mA and 10 °C for 12 h. RT-PCR was carried out from 3 μg of enterocyte (E) or colonocyte (C) total RNAs, under optimal conditions. RT-PCR DNA-bands are designed as E1'–E4' for enterocytes and C1'–C5' for colonocytes. Nested-PCR employed as template 1 μl of 1000-fold dilution of the respective RT-PCR product. Nested-PCR DNA bands are denoted as E1–E4 for enterocytes and C1–C5 for colonocytes. DEPC-treated water was used as negative control (−1). RT-PCR without reverse transcriptase was carried out from enterocyte (E-2) or colonocyte (C-2) RNAs to discard genomic-DNA contamination. DNA fragments were eluted and cloned into pCR4-TOPO plasmid. Inserts were re-amplified from plasmid and analyzed by electrophoresis (right panel). The seven cloned cDNA fragments were denoted as F1–F7. Cloned fragments were sequenced and their sizes are indicated below them. M_{100}: 100-bp DNA Ladder. (B) Table summarizes the characteristics of each cloned cDNA-fragment, including size, origin band, associated ATPase, GenBank Accession Number and genetic analysis through Blast programs.

1D Image Analysis Software v.3.0.2", being the size of each DNA-band calculated. PAGE was run in Protean II xi Cell chamber. Agarose gels were run in Mini-Cell Primo EC320 chamber.

Cloning and sequencing of Nested-PCR products. DNA-fragments were thermo-eluted from 4% PAGE [21] and cloned using TOPO TA Cloning Kit for Sequencing. Addition of A-overhangs and DNA-cloning were carried out following manufacturer instructions. Plasmids were isolated from positive colonies through Wizard Plus SV Minipreps DNA Purification System. To corroborate DNA-inserts, they were re-amplified by repetition of Nested-PCR, employing as template 100 ng of the respective plasmid and analyzed by electrophoresis. DNA-inserts were sequenced by MACROGEN INC. (South Korea) and MACROGEN CORP. (USA) employing the universal-M13 forward and reverse primers. Sequences of both strands were verified with internal primers.

DNA sequence analysis. DNA sequences were compared with GenBank database through "blastn" and "blastx" programs (http://blast.ncbi.nlm.nih.gov/Blast.cgi) and matched with *Cavia porcellus* genome through ENSEMBL Genome database (http://www.ensembl.org/index.html). DNA sequences were translated by "Translate" tool (http://us.expasy.org/tools/dna.html). All analyzed sequences have optimal Q_{16} values.

Results

RT-PCR and Nested-PCR were carried out to identify the expression of P-type ATPase mRNAs, from subtypes II, in intestinal epithelial cells.

Fig. 2A shows the 4% PAGE of RT-PCR and Nested-PCR products from enterocytes (E) and colonocytes (C). Four DNA-bands were detected by RT-PCR in enterocytes (E1'–E4') and five DNA-bands in colonocytes (C1'–C5'). Likewise, Nested-PCR generated four DNA-bands in enterocytes (E1–E4) and five DNA-bands in colonocytes (C1–C5). In general, Nested-PCR bands showed a faster electrophoretic mobility than those observed in RT-PCR products, due to the size-reduction (33 bp) generated by the nesting procedure (as described in Fig. 1C).

Each DNA-band, detected in Nested-PCR, was cut from the gel and the contained-DNA was eluted, cloned and sequenced. Seven different cDNA-fragments were identified (F1–F7). To corroborate the DNA-band of origin, cloned-fragments were re-amplified from plasmid and run beside the Nested-PCR products onto 4% PAGE (Fig. 2A, "Cloned cDNA-fragments" panel). All cloned fragments showed the same electrophoretic mobility than their parental Nested-PCR bands.

The sequence of each cDNA-fragment was compared with those of the GenBank database through BLAST programs. Genetic identity was confirmed by comparison with guinea-pig genomic DNA through ENSEMBL program. Fig. 2B summarizes the characteristics of cloned cDNA-fragments. F1-fragment (980 bp), corresponding to PMCA1, was obtained from the second band of enterocytes (E2) and colonocytes (C2). F2-fragment (974 bp) matches PMCA4 and was only cloned from the enterocytes (E2-band). This preferential expression of PMCA4 in enterocytes was corroborated by RT-PCR (Fig. 3B), where a specific PMCA4-product (279 bp) was clearly detected after 30 cycles in enterocytes, while it was necessary at least 34 cycles to detect it in colonocytes. This difference was quantified by qRT-PCR (Fig. 3C). PMCA4 mRNA was expressed in enterocytes 7.55-fold more than colonocytes ($p < 0.01$). F3-fragment (1037 bp) corresponds to Na^+/K^+-ATPase α1-isoform (ATP1A1) and was obtained from the third band of enterocytes (E3) and colonocytes (C3). Two different cDNA-fragments: F4 (1067 bp) and F5 (1070 bp), corresponding to SERCA2 and SERCA3, respectively, were cloned from the fourth band of both cellular types (E4 and

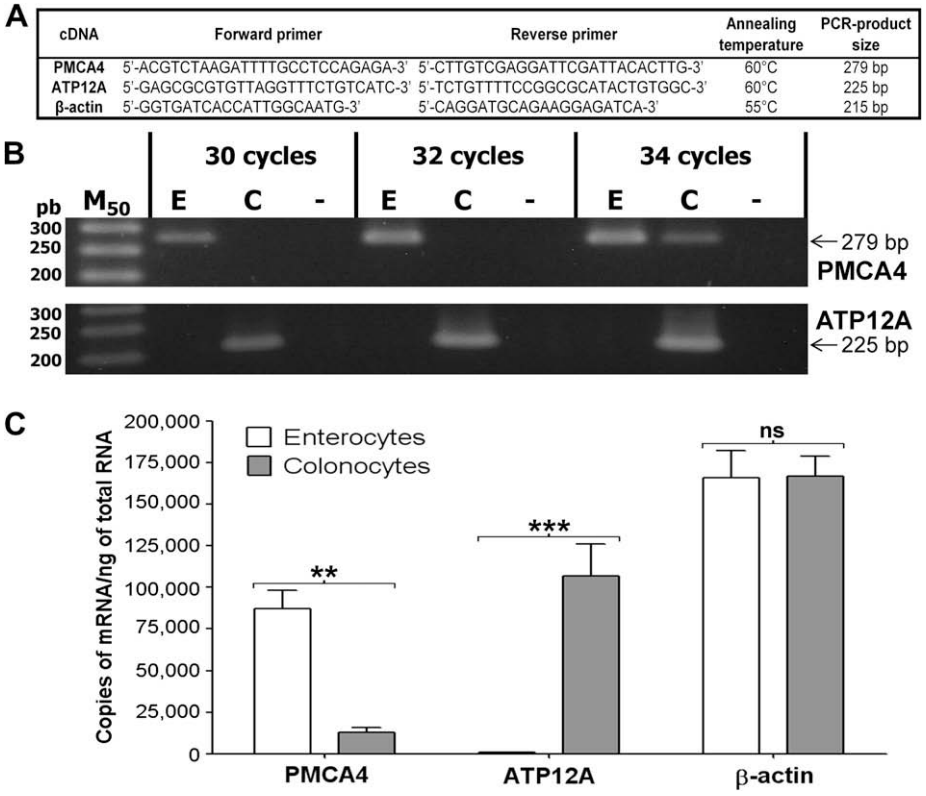

Fig. 3. Quantification of differentially-expressed P-type ATPase mRNAs by qRT-PCR. (A) Specific primers and annealing temperatures employed. (B) RT-PCRs for PMCA4 and ATP12A were carried out from Poly(A)$^+$-RNA of enterocytes (E) or colonocytes (C) and PCR-products were run onto 2% agarose gel electrophoresis. DEPC-treated water was used as negative control (−). Number of PCR-cycles employed is indicated above. M_{50}: 50-bp DNA Ladder. C: Real-time RT-PCRs for PMCA4, ATP12A and β-actin were carried out as triplicate, employing 1 μl of RT-reaction obtained from 3 μg of total RNA. Results are mean ± SEM of three independent experiments. $^{**}p < 0.01$; $^{***}p < 0.001$.

C4). F6-fragment (1037 bp) corresponds to H^+/K^+-ATPase α2-isoform (ATP12A) and was isolated from C5-band, only detected in colonocytes. The exclusive expression of ATP12A in colonocytes was corroborated by RT-PCR and qRT-PCR (Fig. 3B–C). Despite their identical molecular size (1037 bp), ATP12A-fragment showed a slower migration than ATP1A1-fragment in PAGE. Nevertheless, these fragments migrate at the same mobility-rate in agarose gel electrophoresis (Supplementary Figure). It is evident that the paradoxical mobility of ATP12A-fragment is due to an anomalous behavior in PAGE. Finally, a cDNA-fragment of 902 bp, denoted as F7 in Fig. 2, was cloned from the first band of each cellular type (E1 and C1). The sequence of F7-fragment has some similarities with F3-fragment (corresponding to ATP1A1). Fig. 4A shows the schematic alignment between both fragments, which share two lateral segments of 207 and 695 bp, but F7-fragment lacks of a middle segment of 135 bp present in F3-fragment. We denominated this new cDNA-fragment as ATNA to distinguish it from ATP1A1. The 135 bp-segment, present in ATP1A1 but absent in ATNA, encodes 45 amino acids located into the C-loop, between E- and F-motifs. This peptide segment is preserved in all Cation/K^+-ATPases (Fig. 4A). Comparison with ENSEMBL genomic database reveals that 135 bp-segment exactly corresponds to the 11th exon of the guinea-pig *atp1a1* gene (Fig. 4B). ATNA-fragment could correspond to a new cassette-type splice-variant of *atp1a1*, lacking of the 11th exon.

Cloned cDNA sequences have 100% of identity with guinea-pig genomic database, indicating that amplification, electrophoresis, elution and cloning procedures did not introduce any modification into DNA sequences. As expected, the amplification generated specific PCR-product size for each ATPase. The partial cDNA sequences of PMCA1, PMCA4, ATP1A1, SERCA2, SERCA3 and ATNA from guinea-pig are reported for the first time (GI: 170524479, 170524481, 170524495 [bases 439-1475], 170524483, 170524485 and 170524493 [bases 439-1340], respectively).

Discussion

Different P-type ATPase activities, with diverse ion-specificity, affinity, regulation and cell distribution, have been reported in intestinal epithelia [4–8,11–13]. However, some of them have not been associated with a specific gene [7,8]. Until now, 15 genes of P-type ATPases that transport low-atomic-weight cations (Ca^{2+}, Na^+, K^+ and H^+) have been reported in mammalia [2,3]. These enzymes present a tissue-specific distribution with physiological implications [22–24]. The aim of the present work was to define the repertory of P-type ATPases, from subtypes II, expressed in enterocytes and colonocytes, which could partly explain the functional differences existing between them.

Seven P-type ATPase cDNA-fragments were cloned from isolated enterocytes and colonocytes of guinea-pig: PMCA1, PMCA4, SERCA2, SERCA3, ATP12A, ATP1A1 and ATNA (Fig. 2). ATP12A was exclusively detected in colonocytes, while PMCA4 was preferentially expressed in enterocytes. All other cDNAs were identified in both cellular types. SERCA2 and ATNA are reported in intestinal epithelial cells for the first time. Additionally, expression of SERCA3, PMCA1, PMCA4, ATP1A1 and ATP12A in intestinal epithelium was verified [4–6].

The simultaneous expression of different isoforms of SERCA and PMCA in the same cell population does not seem to be redundant

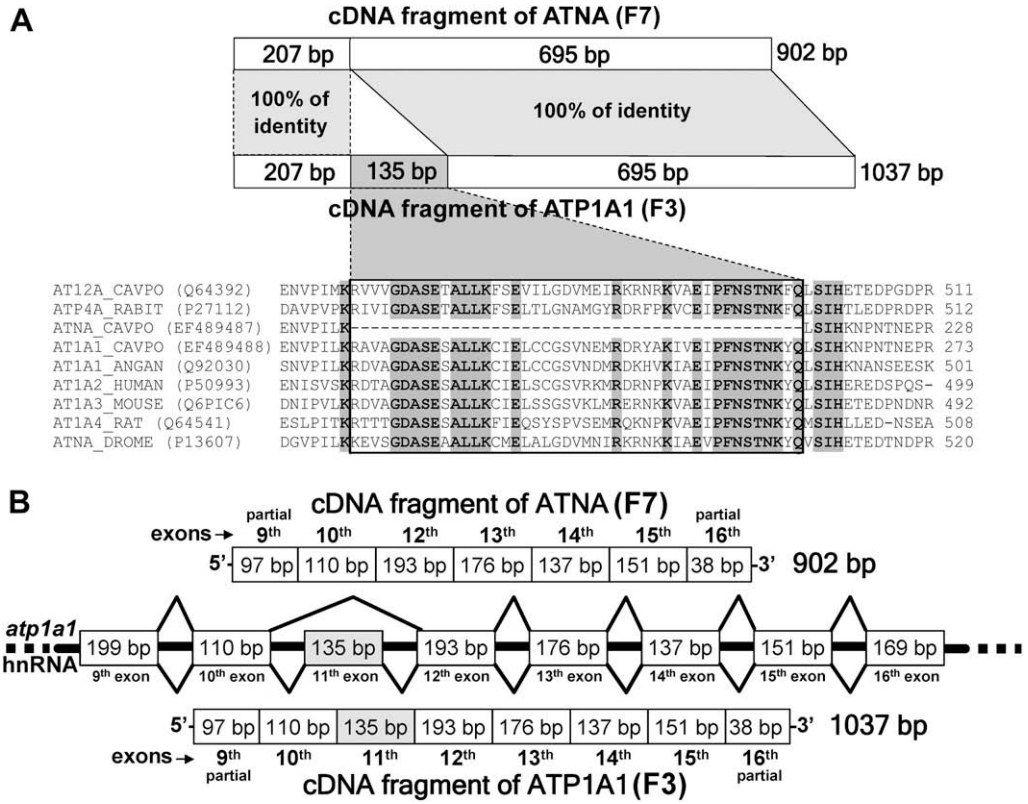

Fig. 4. Comparison of ATNA and ATP1A1 fragments. (A) Schematic alignment of ATNA and ATP1A1 fragments. The segment of 135 bp, present in ATP1A1 but absent in ATNA, is highlight in gray. These cDNA-fragments were translated and aligned with several Cation/K^+-ATPase sequences through ClustalX v1.81 program. The 135-bp segment encodes 45 amino acids, highly-preserved in all Cation/K^+-ATPases (enclosed by a rectangle), which includes 21 residues 100% conserved in this protein group (shadow residues). (B) Exon organization in ATNA and ATP1A1 fragments. The 135-bp segment, missing in ATNA, was identified as the 11th exon of *atp1a1* gen. This exon (highlight in gray) could be alternatively included or excluded during splicing process, generating ATP1A1 or ATNA mRNAs, respectively.

because these isoforms have different properties. SERCA2 is modulated by phospholambam but SERCA3 is not [25,26], likewise PMCA1 and PMCA4 have differences in membrane-targeting and regulation by calmodulin and protein-kinases [22,23,26,27]. Although PMCA1 and PMCA4 are considered ubiquitously distributed [28], PMCA1-expression is considered constitutive, while PMCA4-expression can be regulated by different conditions [28–31]. Colonic-derived HT-29 cultured cells have a low basal PMCA4-expression level that is increased when they are stimulated to differentiate to enterocyte-like cells, producing an increase in active Ca^{2+}-uptake [29]. Similar results have been obtained with other colonic and gastric cancer cultured cells [30]. In addition, stimulation of MDCK monolayers with D_3-vitamin produces an overexpression of PMCA4 (without changes in PMCA1) and concomitantly increases the transepithelial Ca^{2+}-transport from luminal to basolateral side [31]. Furthermore, intestinal Ca^{2+}-absorption, which is dependent of basolateral Ca^{2+}-pumps [32], mainly occurs at proximal intestinal segments [13], where PMCA4 is high-expressed (Fig. 3B–C). In contrast, distal colon, where PMCA4 is low-expressed (Fig. 3B–C), secretes calcium [13]. D_3-vitamin treatment, which induces PMCA4-expression [31], shifts this colonic Ca^{2+}-secretion to net Ca^{2+}-absorption [13]. Thus, differential expression of PMCA4, between enterocytes and colonocytes, could be associated to the regulation of intestinal Ca^{2+}-absorption.

Expression of ATP12A mRNA has been reported in distal colon, kidney, uterus and skin, but not in small-intestine [33,34]. This gene has been associated to the colonic ouabain-sensitive H^+/K^+-ATPase [35], responsible for the apical H^+/K^+-exchange involved in the colonic K^+-absorption [36]. In mammalian gastrointestinal tract, ouabain-sensitive H^+/K^+-exchange and the respective H^+/K^+-ATPase have been only identified in distal colon [37], in agreement with the differential expression of ATP12A mRNA reported in this paper (Fig. 3B–C). Therefore, the selective expression of ATP12A in distal colon must be related with the role of this intestinal segment in the K^+-absorption.

ATNA and ATP1A1 cDNA-fragments differ in a central segment of 135 bp, which is absent in ATNA and corresponds to the 11th exon of guinea-pig *atp1a1* gen. ATNA-fragment could be a new cassette-type splice-variant of *atp1a1* without the 11th exon (Fig. 4B). The functional implications of this exon-missing are unknown and must be evaluated. This fragment matches ATNA-cDNAs of guinea-pig epithelial intestinal cells (GI: 170524493) and dog MDCK cells (GI: 170524491), reported by our laboratory [38]. Expression of ATNA and ATP1A1 in MDCK cells have been quantified by qRT-PCR in 1.53×10^4 and 10.23×10^4 mRNA copies per nanogram of total RNA, respectively [38].

Alternative-splicing is usual in P-type ATPases [22,23,26,27] and similar cassette-type splice-variants have been described for these enzymes. For example, the 19th exon of 154 bp, present in splice-variant 1 of human PMCA1 (GI: 48255946), is missing in splice-variant 2 (GI: 48255944). Until now, three ATP1A1 splice-variants had been reported (GI: 219941, 806751 [39] and 170524497). However, ATNA would be the first reported cassette-type splice-variant of P-type ATPase with changes into C-loop.

Conclusions

Epithelial cells of small intestine and distal colon have functional differences that are partially due to the differential expression of P-type ATPases. Enterocytes, which actively absorb calcium, preferentially expressed PMCA4. In contrast, ATP12A was differentially expressed in colonocytes that actively absorb potassium. Several P-type ATPases are shared by both cellular types, including a putative new splice-variant of *atp1a1* gene.

Acknowledgments

We thank Dr. Howard Takiff, MSc., María Sulbarán, Dr. Flor Pujol and Lic. Carmen Loureiro for their cooperation. This work was supported by Grants from FONACIT (Project Numbers: F-2005000222 and S1-2000000552) and MISIÓN CIENCIA (Project Number: 20070001585).

Appendix A. Supplementary data

Supplementary data associated with this article can be found, in the online version, at doi:10.1016/j.bbrc.2009.11.023.

References

[1] J.V. Møller, B. Juul, M. LeMarie, Structural organization, ion transport and energy transduction of P-type ATPase, Biochem. Biophys. Acta 1286 (1996) 1–51.
[2] W. Kühlbrandt, Biology, structure and mechanism of P-type ATPases, Nat. Rev. Mol. Cell. Biol. 5 (2004) 282–295.
[3] M.G. Palmgren, K.B. Axelsen, Evolution of P-type ATPases, Biochim. Biophys. Acta 1365 (1998) 37–45.
[4] K.D. Wu, W.S. Lee, J. Wey, D. Bungard, J. Lytton, Localization and quantification of endoplasmic reticulum Ca(2+)-ATPase isoform transcripts, Am. J. Physiol. 269 (1995) C775–C784.
[5] A. Howard, S. Legon, J.R. Walters, Human and rat intestinal plasma membrane calcium pump isoforms, Am. J. Physiol. 265 (1993) G917–G925.
[6] F. Jaisser, N. Coutry, N. Farman, H.J. Binder, B.C. Rossier, A putative H^+/K^+-ATPase is selectively expressed in surface epithelial cells of rat distal colon, Am. J. Physiol. 265 (1993) C1080–C1089.
[7] J.R. del Castillo, J.W. Robinson, Na^+-stimulated ATPase activities in basolateral plasma membranes from guinea-pig small intestinal epithelial cells, Biochim. Biophys. Acta 812 (1985) 413–422.
[8] J.R. del Castillo, V.M. Rajendran, H.J. Binder, Apical membrane localization of ouabain-sensitive K(+)-activated ATPase activities in rat distal colon, Am. J. Physiol. 261 (1991) G1005–G1011.
[9] L. Yatime, M.J. Buch-Pedersen, M. Musgaard, J.P. Morth, A.M. Lund-Winther, B.P. Pedersen, C. Olesen, J.P. Andersen, B. Vilsen, B. Schiøtt, M.G. Palmgren, J.V. Møller, P. Nissen, N. Fedosova, P-type ATPases as drug targets: tools for medicine and science, Biochim. Biophys. Acta 1787 (2009) 207–220.
[10] E. Lecuona, H.E. Trejo, J.I. Sznajder, Regulation of Na, K-ATPase during acute lung injury, J. Bioenerg. Biomembr. 39 (2007) 391–395.
[11] H.N. Nellans, S.G. Schultz, Relations among transepithelial sodium transport, potassium exchange, and cell volume in rabbit ileum, J. Gen. Physiol. 68 (1976) 441–463.
[12] J.R. Del Castillo, M.C. Súlbaran-Carrasco, L. Burguillos, K^+ transport in isolated guinea-pig colonocytes: evidence for Na(+)-independent ouabain-sensitive K^+ pump, Am. J. Physiol. 266 (1994) G1083–G1089.
[13] M.J. Favus, Factors that influence absorption and secretion of calcium in the small-intestine and colon, Am. J. Physiol. 248 (1985) G147–G157.
[14] S. Kwork, S.Y. Chang, J.J. Sninsky, A. Wang, Design and use of mismatched and degenerate primers, in: C.W. Dieffembach, G. Dveksler (Eds.), PCR Primer: A Laboratory manual, Cold Spring Harbor Laboratory Press, Woodbury, New York, 1995, pp. 143–145.
[15] M. Shono, M. Wada, Y. Hara, T. Fujii, Molecular cloning of Na(+)-ATPase cDNA from a marine alga, Heterosigma akashiwo, Biochim. Biophys. Acta 1511 (2001) 193–199.
[16] J.R. del Castillo, The use of hyperosmolar, intracellular-like solutions for the isolation of epithelial cells from guinea-pig small-intestine, Biochim. Biophys. Acta 901 (1987) 201–208.
[17] J. Sambrook, E.F. Fritsh, T. Maniatis, Molecullar Cloning: A Laboratory Manual, second ed., vol. 1, Cold Spring Laboratory Editorial, New York, 1989.
[18] X. Yang, J.E. Marchand, Optimal ratio of degenerate primer pairs improves specificity and sensitivity of PCR, Biotechniques 32 (2002) 1002–1006.
[19] K.N. Wada, Y. Wada, H. Doi, F. Ishibashi, T. Gojobori, T. Ikemura, Codon-usage tabulated from the GenBank genetic sequence data, Nucleic Acids Res. suppl. 19 (1991) 1981–1986.
[20] J.D. Thompson, T.J. Gibson, F. Plewniak, F. Jeanmougin, D.G. Higgins, The ClustalX windows interface. flexible strategies for multiple sequence alignment aided by quality analysis tools, Nucleic Acids Res. 24 (1997) 4876–4882.
[21] M.R. Frost, J.A. Guggenheim, Prevention of depurination during elution facilities the reamplification of DNA from differential display gels, Nucleic Acids Res. 27 (1999) e6,i–iv.
[22] D. Guerini, E. Garcia-Martin, A. Zecca, F. Guidi, E. Carafoli, The calcium-pump of the plasma membrane: membrane-targeting, Calcium binding-sites, tissue-specific isoform expression, Acta Physiol. Scand. Suppl. 643 (1998) 265–273.
[23] E.E. Strehler, A.G. Filoteo, J.T. Penniston, A.J. Caride, Plasma-membrane Ca(2+)pumps: structural diversity as the basis for functional versatility, Biochem. Soc. Trans. 35 (2007) 919–922.

[24] E.E. Strehler, D.A. Zacharias, Role of alternative splicing in generating isoform diversity among plasma membrane calcium-pumps, Physiol. Rev. 81 (2001) 21–50.
[25] M. Tada, T. Toyofuku, SR Ca(2+)-ATPase/phospholamban in cardiomyocyte function, J. Card. Fail. 2 (1996) S77–S85.
[26] A.K. Grover, I. Khan, Calcium-pump isoforms: diversity, selectivity and plasticity, Cell Calcium 13 (1992) 9–17.
[27] F. Di Leva, T. Domi, L. Fedrizzi, D. Lim, E. Carafoli, The plasma membrane Ca^{2+}ATPase of animal cells: structure, function and regulation, Arch. Biochem. Biophys. 476 (2008) 65–74.
[28] G.W. Okunade, M.L. Miller, G.J. Pyne, R.L. Sutliff, K.T. O'Connor, J.C. Neumann, A. Andringa, D.A. Miller, V. Prasad, T. Doetschman, R.J. Paul, G.E. Shull, Targeted Ablation of Plasma Membrane Ca^{2+}-ATPase (PMCA) 1 and 4 Indicates a Major Housekeeping Function for PMCA1 and a Critical Role in Hyperactivated Sperm Motility and Male Fertility for PMCA4, J. Biol. Chem. 279 (2004) 33742–33750.
[29] C.S. Aung, W.A. Kruger, P. Poronnik, S.J. Roberts-Thomson, G.R. Monteith, Plasma membrane Ca^{2+}-ATPase expression during colon cancer cell line differentiation, Biochem. Biophys. Res. Commun. 355 (2007) 932–936.
[30] P. Ribiczey, A. Tordai, H. Andrikovics, A.G. Filoteo, J.T. Penniston, J. Enouf, A. Enyedi, B. Papp, T. Kovács, Isoform-specific up-regulation of plasma membrane Ca^{2+}ATPase expression during colon and gastric cancer cell differentiation, Cell Calcium 42 (2007) 590–605.
[31] S.N. Kip, E.E. Strehler, Vitamin-D3 upregulates plasma membrane Ca^{2+}-ATPase expression and potentiates apico-basal Ca^{2+}-flux in MDCK cells, Am. J. Physiol. Renal Physiol. 286 (2004) F363–F369.
[32] F. Bronner, Mechanisms of intestinal calcium absorption, J. Cell. Biochem. 88 (2003) 387–393.
[33] M.S. Crowson, G.E. Shull, Isolation and Characterization of a cDNA Encoding the Putative Distal Colon H^+, K^+-ATPase, J. Biol. Chem. 261 (1992) 13740–13748.
[34] A.V. Grishin, V.E. Sverdlov, M.B. Kostina, N.N. Modyanov, Cloning and characterization of the entire cDNA encoded by ATP1AL1 – a member of the human Na,K/H, K-ATPase gene family, FEBS Lett. 349 (1994) 144–150.
[35] J. Codina, J.T. Delmas-Mata, T.D. DuBose Jr., The alpha-subunit of the colonic H^+, K^+-ATPase assembles with beta1-Na^+, K^+-ATPase in kidney and distal colon, J. Biol. Chem. 273 (1998) 7894–7899.
[36] J.H. Sweiry, H.J. Binder, Active potassium-absorption in rat distal colon, J. Physiol. 423 (1990) 155–170.
[37] K. Kunzelmann, M. Mall, Electrolyte transport in the mammalian colon: mechanisms and implications for disease, Physiol. Rev. 82 (2002) 245–289.
[38] J.R. del Castillo, M.A. Rocafull, F.R. Romero, L.E. Thomas, L. Cariani, Cloning, silencing of the second sodium-pump, FEBS J. 274 (2007) s126.
[39] A. Ruiz, S.P. Bhat, D. Bok, Characterization and quantification of full-length and truncated Na, K-ATPase alpha 1 and beta 1 RNA transcripts expressed in human retinal pigment epithelium, Gene 155 (1995) 179–184.